

Short Communication

## Effect of Niobium Micro-Alloying Addition on Electrochemical Corrosion Behavior of Mild Steel in a Highly Alkaline Environment

Shulong Liu<sup>1</sup>, Chao Gao<sup>1,\*</sup>, Ping Yan<sup>2</sup>

<sup>1</sup> School of Physics and Electronic Information/Information College, Huaibei Normal University, Huaibei, Anhui 235000, P R China

<sup>2</sup> School of Life Science, Huaibei Normal University, Huaibei, Anhui 235000, P R China

\*E-mail: [gaochao@chnu.edu.cn](mailto:gaochao@chnu.edu.cn)

Received: 7 February 2020 / Accepted: 18 March 2020 / Published: 10 May 2020

---

Corrosion behavior of niobium (Nb) micro-alloyed steel in a highly alkaline environment were studied by electrochemical method. Electrochemical characterizations such as electrochemical impedance spectroscopy (EIS), potentiodynamic polarization and cyclic voltammetry (CV) were utilized to consider the Nb addition effect on corrosion resistance of mild steel. The current value decreased to zero potential with the increase of the Nb content in CV curves, which means that the addition of Nb facilitates the formation of stable passive film. The polarization results indicated that the mild steel with 0.03 wt% Nb was in the passive region during the exposure time and had a smaller current than that of other samples. The EIS results indicated that the double-layer capacitance value reduced with the increase of Nb content which revealed that the passive film thickness had increased and resulted in the enhancement of the protective capacity when the Nb content of microalloyed steel was gradually increased. Scanning electron microscopy images indicated that the surface of the steel (0.03 wt% Nb) was clean and smooth without any visible corrosion zones, which means that the sample had a suitable corrosion resistance even in an aggressive environment.

---

**Keywords:** Mild steel; Corrosion behavior; Electrochemical characterizations; Alkaline environment

### 1. INTRODUCTION

Carbon steel reinforced concrete is a material widely used in the construction industry worldwide because of its mechanical resistance and extraordinary structural strength [1]. Corrosion of mild steel is one of the problems in various applications such as electronics, biology and construction industry that need further evaluation to improve the corrosion condition [2-4]. The high corrosion resistance of the alloy is usually due to the formation of a stable passive film produced on its surface

[5]. The passive layer on the surface of carbon steel is stable in the alkaline environment [6]. It seems that the existence of carbonation had caused a uniform passivation of steels because of the  $\text{CO}_3^{2-}/\text{HCO}_3^-$  at a specific pH value [7]. Several environmental factors such as  $\text{NO}_2$  and  $\text{SO}_2$  in acid rain and  $\text{CO}_2$  in the air pollutions lead to the reduction of environment alkalinity [8, 9]. Today, low-alloy steel are alternative techniques to promote corrosion resistance. Niobium (Nb) is one of the elements employed in low-alloy steel. Xu et al. [10] showed that the  $\text{Ti}_5\text{Si}_3$  corrosion resistance was promoted with the increase of Nb content in  $\text{H}_2\text{SO}_4$  solution. Sun et al. [11] suggested the addition of Nb in steel can lead to a satisfactory performance to enhance the corrosion resistance of stainless steel. OrjuelaG et al. [12] had improved the corrosion resistance by coating niobium carbide on the surface of low-alloy steel. Many researches were focused on the study of Nb effect on steel in acidic environments [13]. However, studies in the alkaline environment by the electrochemical process have not been published yet. Therefore, in this work, the effect of Nb content on mild steel corrosion in an alkaline environment (pH value of 12) were investigated. The cyclic voltammetry, electrochemical impedance spectroscopy and potentiodynamic polarization techniques were utilized to study the electrochemical properties of Nb microalloyed HRB500 mild steel in a highly alkaline solution.

## 2. MATERIALS AND METHOD

Experimental materials were alloy corrosion-resistant HRB400 steel with diameter of 20 mm in alkaline environment. Table 1 presents the chemical composition of the four kinds of mild steels used in this study.

**Table 1.** Chemical composition of Nb microalloyed HRB500 mild steel (wt%)

Alloys	C	Mn	Si	P	S	Nb	Fe
Mild steel	0.25	1.55	0.50	0.03	0.025	0.0	Residual
0.02 wt% Nb	0.24	1.55	0.53	0.03	0.025	0.020	Residual
0.025 wt% Nb	0.24	1.55	0.50	0.03	0.025	0.025	Residual
0.03 wt% Nb	0.24	1.55	0.50	0.03	0.025	0.030	Residual

The Nb additions are set from 0.0 wt% to 0.03 wt%. Silicon carbide papers down to 2500# (LANHU, Germany) were employed to polish the samples. All samples were cleaned in acetone in an ultrasonic cleaner (Mophorn, China) and washed in distilled water.

The alkaline environment was prepared using  $5 \text{ g L}^{-1}$  of KOH,  $0.75 \text{ g L}^{-1}$  NaOH, and  $0.75 \text{ g L}^{-1}$   $\text{Ca}(\text{OH})_2$ . The mass fraction of NaCl in the solution was 1.0 wt%. The pH of solutions was adjusted by adding an amount of  $\text{NaHCO}_3$  in 12.0 and calibrating by a pH meter.

The homemade electrochemical cell was used to study on the electrochemical impedance spectroscopy (EIS) of the samples. In the three-electrode system, steel samples were used as a working electrode and a saturated calomel electrode was applied as a reference electrode. The graphite was used as the counter electrode. Before analysing the samples, all samples were immersed in a prepared solution for 25 minutes. A copper wire was connected to the ends of the steel samples. EIS

characterizations were performed in the frequency varied between 100 kHz and 0.1 mHz at the  $E_{OC}$  with AC perturbation  $\pm 10$  mV. The potentiodynamic polarization (CorrTest Instruments Corp., Ltd., China) measurement was conducted from 0.25V at 1 mV/s scanning rate. The cyclic voltammetry analysis was carried out between -1.5V and 1.5 V at scan rate with 50 mV/s and recorded sixth cyclic voltammograms in order to make comparison between samples. The morphology of the samples was analyzed by scanning electron microscopy (SEM, FEI Sirion 200).

### 3. RESULTS AND DISCUSSION

In order to study the redox reactions and the formation of the passive layer on the sample in the alkaline environment, cyclic voltammetry (CV) technique was used [14]. Figure 1 shows the cyclic voltammograms of the samples in the alkaline solution with pH value of 12. The anodic and cathodic peak potentials can be observed in Figure 1.

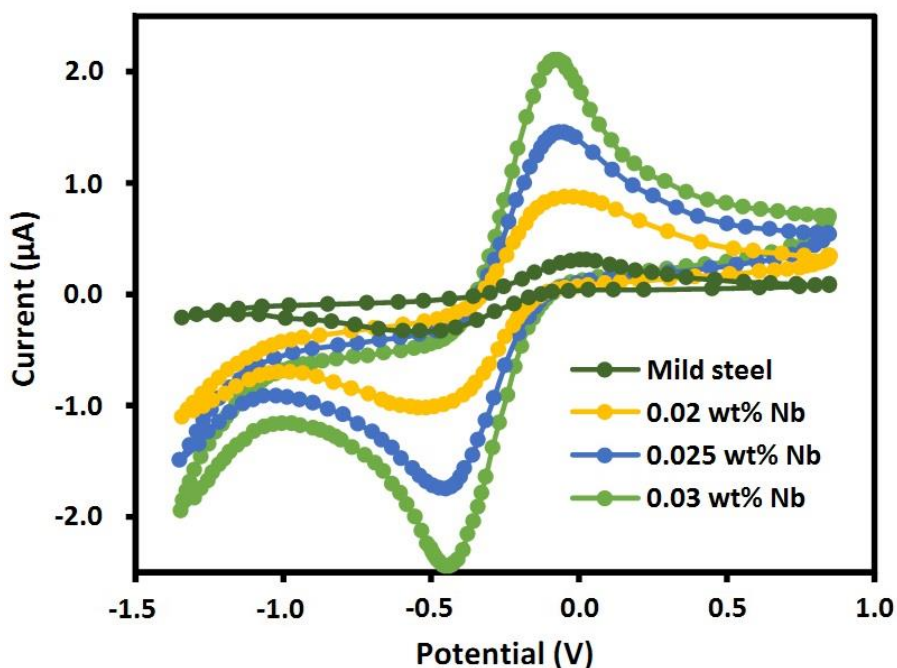


**Figure 1.** Cyclic voltammograms of the samples with different Nb content exposed to the alkaline solution with pH value of 12.

The anodic peaks appeared at approximate potential of -0.25 V for all samples that can be related to the following reactions from (1) to (3). These results confirm the transformation from  $Fe^{2+}$  to  $Fe^{3+}$  ions and the passive layer formation on the surface of steels [15]:



As previously reported, the current density in zero potential ( $i_0$ ) can exhibit the corrosion behavior of the passive layer [16]: the higher  $i_0$  proposes poorer corrosion resistance. When Nb content

increases,  $i_0$  decreases. This reduction indicates that a small amount of Nb micro-alloy in steel facilitates the stability of the formed passive layers. As the potential increases up to 0.1 V, the anodic current-density suddenly increases which can be related to the electrochemical process controlled by the oxygen evolution. As shown in figure 1, the cathodic peak appears at the potential of -0.45 V. When the potential shifts to a more negative value, the cathodic current density increased rapidly which can be associated to the electrochemical process controlled by the hydrogen evolution. Furthermore, the anodic peak of 0.03 wt% Nb steel is lower than other samples. It can be concluded that the increasing Nb content in steel can enhance the corrosion resistance and stability of the passive film [17].

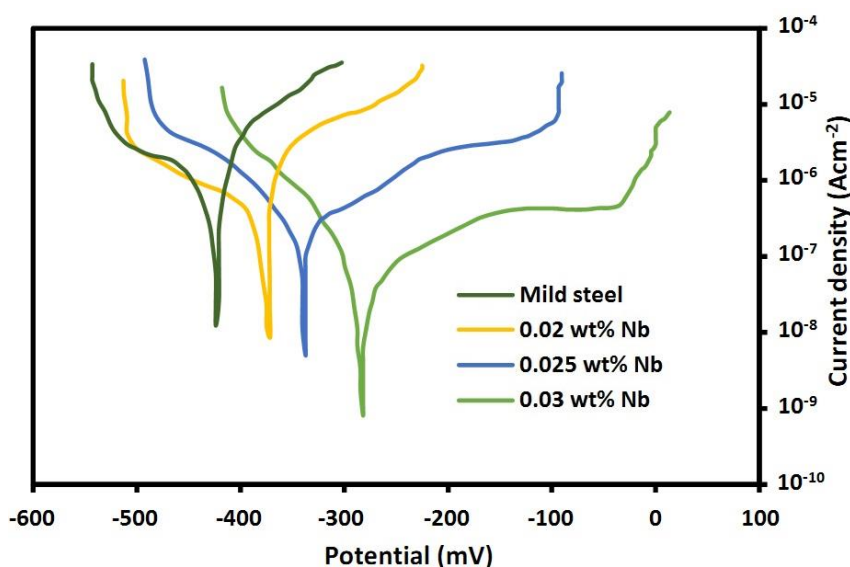


**Figure 2.** Potentiodynamic polarization plots of the samples with different Nb content exposed to the alkaline solution with pH value of 12.

Potentiodynamic polarization method is a conventional electrochemical technique to determine the corrosion rate of the samples. From polarization plots in Figure 2, sample with 0.03 wt% Nb content shows noticeable passivation in the solution and the most positive in pitting potential.

These parameters can be estimated by a curve-fitting method in the weak-polarization behavior for the samples [18]. The value of parameters are summarized in Table 2.

**Table 2.** Fitting parameters of the samples obtained from polarization plots.

Alloy	Corrosion current density ( $\mu\text{Acm}^{-2}$ )	Corrosion potential (mV)	$-\beta_a$ ( $\text{mVdec}^{-1}$ )	$\beta_c$ ( $\text{mVdec}^{-1}$ )
Mild steel	3.21	-422	24	55
0.02 wt% Nb	0.965	-373	28	61
0.025 wt% Nb	0.845	-336	32	59
0.03 wt% Nb	0.098	-285	37	57

Furthermore, the anodic Tafel slope ( $\beta_a$ ), the cathodic Tafel slope ( $\beta_c$ ) as well as the corrosion current density were determined from the Tafel extrapolation method [19]. As shown in table 2,  $\beta_a$  and  $\beta_c$  values change with the concentration of Nb. The change in Tafel slope values can be used to identify the inhibition mechanism (anodic or cathodic) for the carbon steel, the concentration of the electrolyte, the composition of the working electrode and charge transfer coefficient [20]. The values of the cathodic Tafel slopes, significantly unchange with the Nb addition, which implies that its influence on the cathodic reaction does not modify the mechanism of hydrogen evolution discharge [21]. Nevertheless, the values of the slopes of the anodic Tafel lines, change significantly with the addition of Nb suggesting that there were blockage at the anodic reaction sites, and thereby affect the anodic reaction mechanism. Furthermore, with the increase of Nb element, the anode Tafel slope increases which means Nb element could promote the corrosion resistance of steels in alkaline environment.

The corrosion level can be defined into four levels as proposed by Durar Network Specification [22]: very high corrosion for  $1.0 \mu\text{A}/\text{cm}^2 < i_{\text{corr}}$ , high corrosion for  $0.5 \mu\text{A}/\text{cm}^2 < i_{\text{corr}} < 1.0 \mu\text{A}/\text{cm}^2$ , low corrosion for  $0.1 \mu\text{A}/\text{cm}^2 < i_{\text{corr}} < 0.5 \mu\text{A}/\text{cm}^2$ , and passivity for  $i_{\text{corr}} < 0.1 \mu\text{A}/\text{cm}^2$ . According to Table 2, the steel with 0.03 wt% Nb content had a smaller corrosion-current density than the other samples which was in the passive state during the test.

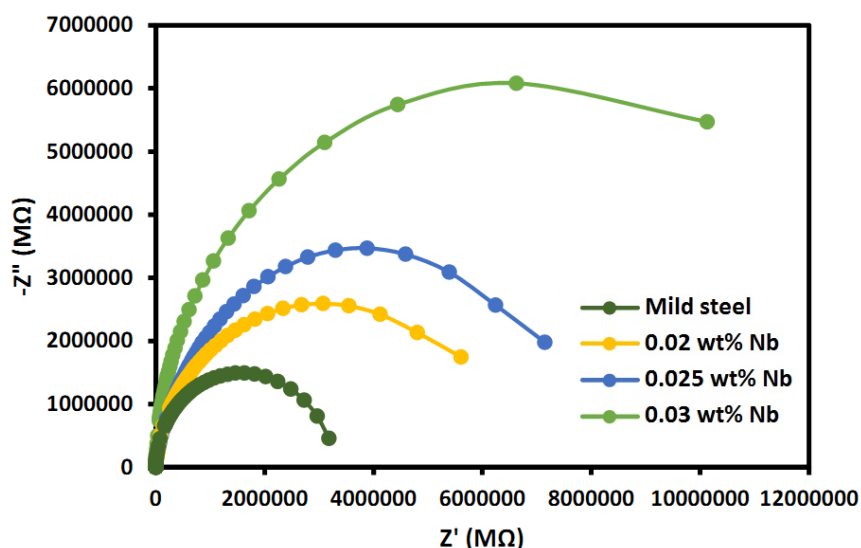


**Figure 3.** Nyquist diagram of the samples with different Nb content exposed to the alkaline solution with pH value of 12.

EIS technique was used to analyze the effect of Nb micro-alloy amount on the corrosion behavior of steels with passive layers in alkaline solution [23]. Figure 3 indicates Nyquist plots of the samples. Two arcs at low and high frequencies appear in Nyquist plots [24]. These are due to the two constant times of reactions occurring on the steel surface. The increase in Nb content leads to an increase in the radius of the capacitive loop which indicates enhancement of the corrosion resistance

for mild steel. The circuit revealed in Figure 4 was used to model the parameters found in the analyzed system.  $R_s$  is the solution resistance. During the passivity period, the second time constant parameters becoming visible at the low frequencies ( $R_{ct}$ ,  $CPE_{dl}$ ) which were associated to the charge transfer resistance and non-ideal interfacial capacitance of the steel surface that revealed the corrosion resistance of the steel surface controlled through the properties of passive film [25]. The first time constant parameters becoming visible at the intermediate frequencies ( $R_f$ ,  $CPE_f$ ) appeared to be correlated with a redox transformation of the corrosion products that occurred on the oxide film surface [26].

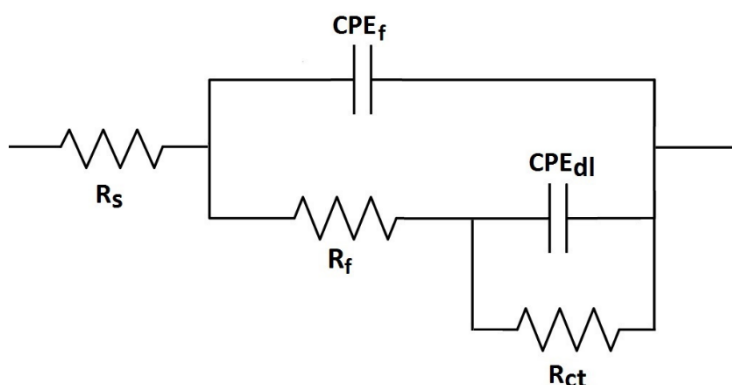


Figure 4. An equivalent circuit model to fit the experimental data

Polarization resistance,  $R_p$  ( $R_p = R_f + R_{ct}$ ) is an assessable indicator to study the corrosion resistance of carbon steel in the corrosive environment. It was noted that the higher  $R_p$  value indicated higher corrosion resistance of the sample.

Table 3. Electrochemical parameters from the fitting using the equivalent circuit in Figure 2 for various content of Nb

Alloy	$R_s$ ( $\Omega \text{ cm}^2$ )	$R_f$ ( $M\Omega \text{ cm}^2$ )	$CPE_f$ ( $\mu\text{F cm}^{-2}$ )	$R_{ct}$ ( $M\Omega \text{ cm}^2$ )	$CPE_{dl}$ ( $\mu\text{F cm}^{-2}$ )
Mild steel	57.6	2.15	3.5	3.37	4.4
0.02 wt% Nb	73.1	3.47	3.2	7.28	3.7
0.025 wt% Nb	59.6	4.93	2.8	8.84	3.3
0.03 wt% Nb	74.6	7.86	2.4	16.92	2.7

According to table 3, increasing the Nb contents show a significantly enhancement in  $R_p$  value indicating a higher corrosion resistance for 0.03 wt% Nb steel in pH 12.

The thickness of the passive film may be determined with the following equation [27]:

$$D = \frac{\epsilon \epsilon_0 A}{Q} \tag{5}$$

Where  $D$  is the passive film thickness,  $\epsilon_0$  ( $8.85 \times 10^{-12} \text{ F m}^{-1}$ ) and  $\epsilon$  (12 for Fe oxides) are the vacuum permittivity and dielectric constant, respectively.  $A$  and  $Q$  are an effective area and capacitance, respectively.

As shown in table 3, the value of  $CPE_{dl}$  (Q) decreases as the Nb content increases, which reveals that the passive film thickness was increased and the resulting protective capacity was enhanced when the Nb content of steel was gradually increased. In pH value of 12, the  $R_f$  passive film resistance increased as the Nb content in alloy increased, which indicated that the protective feature of the passive film developed was strong. Comparing  $CPE_f$  and  $CPE_{dl}$ , it was found that  $CPE_f$  was lower than  $CPE_{dl}$  which confirmed that the formation of the thin passive film and the double layer at the interfaces had a high capacitive behavior.

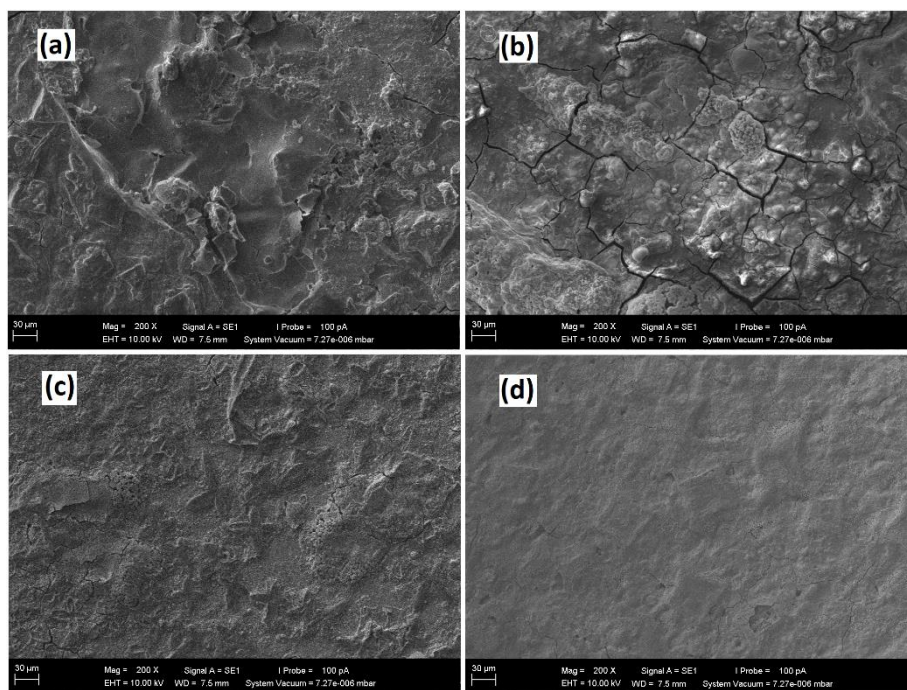


**Figure 5.** SEM images of the samples with different content of Nb, (a) 0 wt% (b) 0.02 wt% (c) 0.025 wt% (d) 0.03 wt%

Figure 5 indicates the SEM images of samples after being exposed to the alkaline solution at 12 pH value for 4 weeks. Extensive corrosion occurs on the surface of samples with 0 wt% and 0.02 wt% Nb content, demonstrating the active corrosion state. Furthermore, few small pits appeared on the surface of sample with 0.025 wt% Nb, and the surface of sample with 0.03 wt% Nb was clean and smooth without any visible corrosion zones, which means these samples had suitable corrosion resistance even in an aggressive environment. These findings reveal that the addition of Nb enhances the corrosion resistance and it is in agreement with the results of electrochemical measurements.

#### 4. CONCLUSIONS

In this work, HRB500 mild steel with 25 mm diameter were used to study the corrosion behavior of Nb microalloyed steel in the alkaline solution. SEM images indicate that the surface of steel with 0.03 wt% Nb is clean and smooth without any visible corrosion zones, which means that the sample has a suitable corrosion resistance even in an aggressive environment. According to

polarization plots, the steel with 0.03 wt% Nb content had a smaller corrosion current-density than the other samples which were in the passive state during the test. The CV results show that the current density in zero potential decreases by increasing the Nb content, indicating a small amount of Nb microalloy in steels facilitates the stability of the formed passive layers. The EIS results indicate that the increase in Nb content leads to an increase in the radius of the capacitive loop which indicates an enhancement of the corrosion resistance for the steel.

#### ACKNOWLEDGEMENT

This work was sponsored in part by Ministry of Education Industry-Academic Cooperative Education (201802327021), Natural Science Foundation of Anhui Higher Education Institutions of China (KJ2015A314), Collaborative Innovation Center of Advanced Functional Materials (XTZX103732016005), Quality engineering at school level (2017jxcg01 and 2019cgj110).

#### References

1. S.A. Umoren, M.M. Solomon, I.B. Obot and R.K. Sulieman, *Journal of Industrial and Engineering Chemistry*, 76 (2019) 94.
2. A. Dutta, S.K. Saha, P. Banerjee and D. Sukul, *Corrosion Science*, 98 (2015) 541.
3. A. Mohammadian, R. Rashednia, G. Lucier, R. Seracino and M. Pour-Ghaz, *Cement and Concrete Composites*, 103 (2019) 263.
4. F. Husairi, J. Rouhi, K. Eswar, A. Zainurul, M. Rusop and S. Abdullah, *Applied Physics A*, 116 (2014) 2119.
5. X. Cheng, H. Luo, K. Xiao and C. Dong, *International Journal of Electrochemical Science*, 12 (2017) 8006.
6. M. Mancio, G. Kusinski, P. Monteiro and T. Devine, *Journal of ASTM International*, 6 (2009)
7. M.B. Valcarce and M. Vázquez, *Materials Chemistry and Physics*, 115 (2009) 313.
8. M. Pandiarajan, P. Prabhakar and S. Rajendran, *European Chemical Bulletin*, 1 (2012) 238.
9. S. Kakooei, H.M. Akil, A. Dolati and J. Rouhi, *Construction and Building Materials*, 35 (2012) 564.
10. J. Xu, L. Liu, I. Zhengyang, P. Munroe and Z.H. Xie, *Acta Materialia*, 63 (2014) 245.
11. T. Sun, B. Deng, J. Xu, J. Li and Y. Jiang, *Journal of Chinese Society for Corrosion and Protection*, 30 (2010) 421.
12. A. OrjuelaG, R. Rincón and J.J. Olaya, *Surface and Coatings Technology*, 259 (2014) 667.
13. J. Rouhi, C.R. Ooi, S. Mahmud and M.R. Mahmood, *Materials Letters*, 147 (2015) 34.
14. F. Husairi, J. Rouhi, K. Eswar, C.R. Ooi, M. Rusop and S. Abdullah, *Sensors and Actuators A: Physical*, 236 (2015) 11.
15. E. Volpi, A. Olietti, M. Stefanoni and S.P. Trasatti, *Journal of Electroanalytical Chemistry*, 736 (2015) 38.
16. C. Wang, S. Yang, Y. Chen, B. Wang, J. He and C. Tang, *RSC Advances*, 5 (2015) 34580.
17. R. Dalvand, S. Mahmud and J. Rouhi, *Materials Letters*, 160 (2015) 444.
18. J.W. Wu, D. Bai, A. Baker, Z.H. Li and X.B. Liu, *Materials and corrosion*, 66 (2015) 143.
19. A. Goyal, H.S. Pouya, E. Ganjian, A.O. Olubanwo and M. Khorami, *Construction and Building Materials*, 194 (2019) 344.
20. Y. Zhou, S. Xu, L. Guo, S. Zhang, H. Lu, Y. Gong and F. Gao, *RSC Advances*, 5 (2015) 14804.
21. A. Ansari, M. Znini, I. Hamdani, L. Majidi, A. Bouyanzer and B. Hammouti, *Journal of Materials and Environmental Science*, 5 (2014) 81.
22. R. Galván-Martínez, C. Gaona-Tiburcio and F. Almeraya-Calderón, *International Journal of Electrochemical Science*, 11 (2016) 2994.

23. J. Rouhi, S. Kakooei, M.C. Ismail, R. Karimzadeh and M.R. Mahmood, *International Journal of Electrochemical Science*, 12 (2017) 9933.
24. H. Liang, S. Li, Y. Lu, J. Hu and Z. Liu, *Composite Structures*, 207 (2019) 576.
25. H. Luo, C. Dong, X. Li and K. Xiao, *Electrochim. Acta*, 64 (2012) 211.
26. A. Bautista, A. González-Centeno, G. Blanco and S. Guzmán, *Mater. Charact.*, 59 (2008) 32.
27. V. Maurice, H. Peng, L.H. Klein, A. Seyeux, S. Zanna and P. Marcus, *Faraday discussions*, 180 (2015) 151.

© 2020 The Authors. Published by ESG ([www.electrochemsci.org](http://www.electrochemsci.org)). This article is an open access article distributed under the terms and conditions of the Creative Commons Attribution license (<http://creativecommons.org/licenses/by/4.0/>).